Combined Aperture for Radio and Optical Communications for Deep Space Links

G.C. Gilbreath,[1] M.A. Rupar,[1] C.O. Font,[1]
and R.C. Romeo[2]
[1]*1nformation Technology Division*
[2]*Composite Mirror Applications, Inc.*

Introduction: To save mass, reduce "wallplug" power, and potentially reduce complexity while increasing communications bandwidth, we consider the feasibility of using a shared aperture for radio frequency (RF) and optical communications. When constructed with composite materials and efficient coatings matched to the wavelengths of interest, we can expect at least an order of magnitude reduction in mass for the communications terminal, which will also enable the use of bandwidths that will support an increase of two orders of magnitude in data rate. NRL evaluated three antennas that could be converted into a dual-use antenna/telescope. We postulated the use of 36 GHz to 38 GHz in the K_a band and 1550 nm in the short wave infrared (SWIR). We compared placement of the secondary for either a shared aperture in the feed train or as part of a bent Cassegrain. The point designs enabled an engineering evaluation of feasibility. We considered adapting a 34-cm spiderless aluminum primary, a 38-cm silver-coated aluminum primary using a spider to hold the subreflector, and the 3-m primary used in the Mars Reconnaissance Orbiter mission. The three baseline structures are shown in Fig. 1.

Coatings: Before proceeding to the architecture itself, we considered coatings that can usefully reflect/transmit K_a while transmitting/reflecting SWIR wavelengths. Three likely candidates for common reflectance are aluminum, silver (to include coated silver), and gold. When considering reflectance at GHz frequencies, the key parameter is skin depth. The measure of reflectance is derived from this basic parameter and is usually estimated based on at least a factor of 2 multiplier. Since a typical thickness of a coating is on the order of 2 to 3 μm, conservative reflectance estimates between aluminum, silver, and gold are nearly equivalent (96.3% for aluminum, 95% for silver, and 95.4% for gold). The driver then becomes response in the SWIR. Equivalent reflectances in the SWIR are 97% for aluminum, 99.4% for silver, and 99% for gold. A coated silver coating may give the best response for a shared aperture. Bare metallic silver adheres weakly to glass and tarnishes when exposed to the atmosphere. The Denton FSS-99 coating, which is a SiO_2 coating, offers 99% reflectance in the infrared and slightly less in the GHz regime. Importantly, all three coatings have been space-qualified for different designs and some have been qualified on carbon reinforced fiber polymer (CFRP) composites.

Aperture/Feed Sharing: How to split the energy is a key question in the design of a shared RF-optical system. There are many ways to approach the problem. In our simple point design, we assume a shared aperture to illustrate use of coatings, unique shared aperture elements, and potential use of composites for the

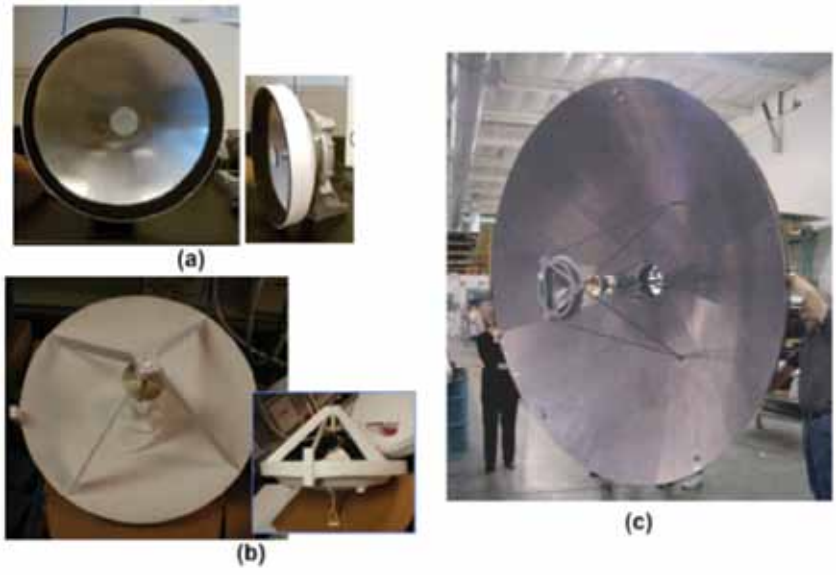

FIGURE 1
Basic structures considered for adaptation to E-O: (a) 34-cm spiderless K_a antenna; (b) 38-cm K_a antenna using spider-mounted subreflector; (c) Mars Reconnaissance Orbiter 3-m high-gain antenna (HGA) and its X-/K_a-band feed (Ref. 1).

structure. First, we assumed use of an antenna primary whose surface is covered with coated silver. This antenna structure now can serve as the telescope primary as well. The K_a energy is received by the antenna and the energy is directed to the subreflector located at the K_a focal point. The energy is reflected from the subreflector to the feed at the center of the antenna in a standard Cassegrain configuration. Similarly, the SWIR energy (1550 nm) is collected by the coated antenna, which we would now call the telescope. At this point, we have several choices. Among them, we can:

(1) Share a common feed aperture
(2) Bend the SWIR out of the feed train (bent SWIR Cassegrain)
(3) Bend the K_a out of the feed train (bent RF Cassegrain)

The shared aperture design is extensively described in literature and is not discussed here. We address the bent Cassegrain designs. In Fig. 2(a), the SWIR is bent from the common beam before the feed. It is directed to an off-axis optical collection path to direct the light to the detectors and electronics. The key element here is a dichroic element that can efficiently reflect 1550 nm and pass 34 to 36 GHz (K_a bands of choice). An alternative configuration is to pass the SWIR through to the optical feed at the center of the primary and bend the K_a energy via a wire mesh element. The mesh can successfully redirect the K_a and pass the SWIR. A G200 wire with 200 μm spacing will allow greater than 95% transmittance at 1550 nm and 99% reflectance at K_a. Although the SWIR efficiency may be impacted by diffraction and some obscuration, a more careful analysis will show that the impact will be on the order of 0.1 dB, if that. A more detailed sketch of this idea is shown in Fig. 2(b), which was offered by Composite Mirror Applications, Inc. as a point design for the concept.[1] Using a wire mesh as a beam dichroic does impose a polarization constraint on a design. That is, one polarization in the RF band is passed and the other is not. Therefore, to maximize efficiency, this must be taken into account when splitting the energy.

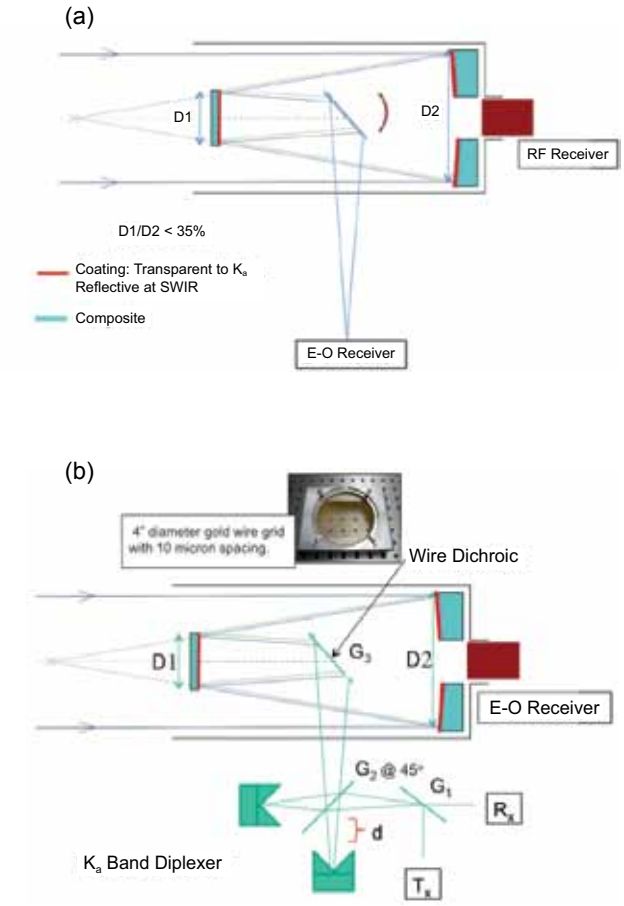

FIGURE 2
(a) Point design is shown to demonstrate how RF can be split from the energy train for a bent Cassegrain shared RF-SWIR aperture. The wire mesh in this case would transmit 1550 nm and pass K_a. (b) Point design is shown to demonstrate how E-O can be split from the energy train for a bent Cassegrain shared aperture. The dichroic in this case would reflect 1550 nm and pass both polarizations of K_a.

Composites: Reducing size, weight, and power (SWAP) of a host platform and its integrated payload is an overarching goal for space applications in particular. Reduction in mass can go a long way in the reduction of power requirements, which in turn further reduces weight and size. Composites, therefore, are of keen interest to the community. Thus, in addition to selection of an architecture where coatings and components are creatively integrated into an effective shared system, the use of composites for the structures themselves were considered. We specifically postulated the use of CFRP. This material has been used to manufacture telescopes and optical telescope assemblies for different architectures and for low-cost replicates. Off-axis aperture sharing, bent beams, and other possibilities will require a structure that is strong, lightweight, and lends itself to customized designs. CFRP can be constructed to roll and unroll for stowage and straightforward deployment. This latter feature is important for space applications.

The CFRP optics and optical train assemblies (OTAs) are at least an order of magnitude lighter than similar telescopes made using traditional glass with aluminum assemblies. CFRP structures are at least 50% lighter than their all-aluminum equivalents. Additionally, the stiffness-to-weight ratio of CFRP is about five times greater than that of steel, the Young's modulus similar, and the density much lower. Thus, stiff, lightweight structures are possible. In addition, the coefficient of thermal expansion for CFRP is very low at 1 to 2 ppm, roughly 20 times lower than for aluminum. For this reason, CFRP structures do not deform with

TABLE 1 — Densities Compared for Some Candidate Materials

Material	Areal Density kg/m^2	Density kg/m^3
Aluminum		2900
Silicon Carbide	32.0	3200
CFRP	5.5	1600
ULE Glass	10.0	2210
Zerodur Glass	45.0	2530

temperature changes. Also, the thermal conductivity of CFRP is similar to that of steel. This property, coupled with the lower mass of a CFRP structure, means that telescope components rapidly equilibrate to their surroundings, which reduces image distortion. Table 1 compares areal densities and volumetric densities for some candidate materials.

Candidate Implementation: When we combine coatings, composites, and unique shared apertures, we can eliminate one primary at a minimum. We further decrease mass by replacing the antenna/telescope assembly structure with composites and enable larger, lighter weight optical telescopes that can also support K_a radio transmissions. When applied to the 3-m high-gain antenna (HGA) used in the Mars Reconnaissance Orbiter, we can offer an efficient 3-m telescope at each end of a Mars–Earth orbiting link that can support the commensurate increase in data rates for both K_a and SWIR-based communications. Top-level link analysis suggests that the data throughput can be increased over baselined X-/K_a-band of 6 Mbps (near Earth) and 500 kbps (furthest from Earth) to multiple Gbps to ~300 Mbps using SWIR. Further efficiencies can be achieved with smart modems that would sense when the optical link is in play and put the RF link in hibernate mode to reduce power draws.[2] This scenario will result in a smaller power loading requirement, further reducing SWAP for the system. Pointing, acquisition, and tracking is assumed to be ideal for these trades. A more sophisticated treatment of the links can be found in Ref. 3.

Implications: The results of this study have been combined with the analyses of other national labs and are being considered by NASA for a Pre-Flight Phase A Study for future Deep Space Missions.

[Sponsored by NASA]

References

[1] G.C. Gilbreath, M.A. Rupar, C.O. Font, and R.C. Romeo, "Combined RF and EO Aperture Study," NRL Report to NASA, September 2010; NRL Formal Report in preparation.
[2] D.S. Kim, G.C. Gilbreath, J. Doffoh, C.O. Font, and M. Suite, "Hybrid Free-space Optical and Radio Frequency Switching," *Proc. SPIE* **7091**, 70910X–70910X-9 (2008).
[3] H. Hemmati, ed., *Near-Earth Laser Communications* (CRC Press, Boca Raton, Fla., 2009).

Goal-Driven Autonomy

D.W. Aha,[1] M. Molineaux,[2] and M. Klenk[3]
[1]*Information Technology Division*
[2]*Knexus Research Corporation*
[3]*Palo Alto Research Center*

Introduction: The Navy needs autonomous intelligent agents to help dominate the battlespace in several types of missions. For example, agents could reduce the amount of warfighter oversight required to operate unmanned vehicles, serve as proactive decision support assistants in C2 systems, and increase the realism of decision-making behaviors for simulated units in training and wargaming systems. However, current-generation agents are severely limited; they must be told how to behave in all situations that they will encounter, or be supervised continuously. Unfortunately, such knowledge engineering is impossible for their complex military environments, which are characterized by incomplete knowledge of the situation, dynamic situation updates, multiple adversaries, and stochastic agent actions. Thus, current agent deployments are highly constrained (e.g., they are programmed to withdraw and report to their operators when any unexpected situations occur).

To achieve full autonomy, agents should dynamically reason about what goals they should pursue to optimize mission performance measures. This will allow them to respond intelligently to unexpected situations as the battlespace situation evolves. We refer to this process as goal reasoning, and next describe our progress on defining a model for it, an agent implementation, and its evaluation.

Model: Figure 3 displays our novel computational model of goal reasoning, also called goal-directed

autonomy (GDA). GDA permits agents to select their goals throughout their deployment (under mission constraints). It extends the controller of the existing model for online planning, which envisions (1) a plan generator, (2) a controller that feeds the plan's actions to the environment, and (3) the environment itself, which uses a function to compute state updates from executing specific actions. A GDA agent monitors a

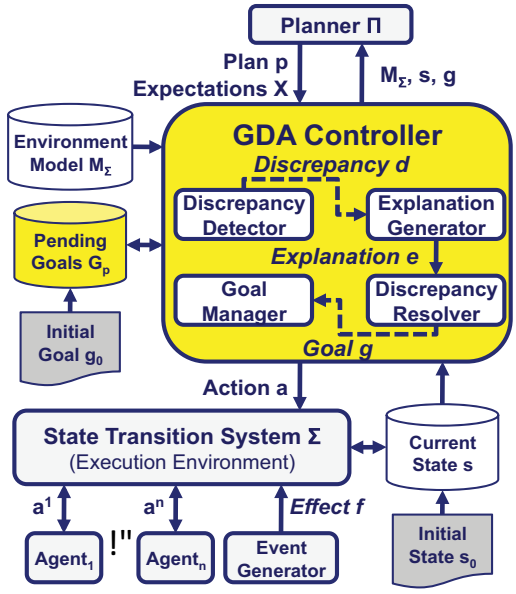

FIGURE 3
Conceptual model for goal-driven autonomy.

plan's execution, and continually compares the current and expected situations (or states). If a discrepancy is detected, then it will generate an explanation of its cause. This is given to a discrepancy resolution module, which may decide to formulate a new goal in response. Finally, a goal manager prioritizes and selects a set of (potentially new) goals to pursue, which are given to the planner to create new plans to execute.

GDA is a general model; many inferencing algorithms could be used for each GDA step. Below we describe one of our instantiations and its empirical investigation.

Implementation and Evaluation: Can the GDA model's additional complexity yield quantifiable benefits? Our hypothesis was that when scenarios produce states that require a GDA agent to change its goals to perform well, it should outperform agents that cannot change their goals. We assessed this by implementing this model in the ARTUE (Autonomous Response to Unexpected Events) agent and comparing its performance vs ablated versions in scenarios defined using complex simulation environments.[1] ARTUE is a simple GDA instantiation; it defines discrepancies as any differences between the expected and actual states, it uses an augmented truth-maintenance system to generate explanations, a set of simple rules to trigger the formulation of goals with specified priorities, and always directs planning to the goal with the highest priority.

For some of our studies, we tested ARTUE using the Tactical Action Officer (TAO) Sandbox, which is a comprehensive littoral simulator used to train TAOs at the Surface Warfare Officers School. We modified the Sandbox such that ARTUE assumes the trainee's interactive role and controls a set of assets (e.g., ship, air, sensors) in antisubmarine and related mission scenarios. For example, the SubHunt scenario involves a search for an enemy submarine that has been spotted nearby. A ship is dispatched to locate and engage it. However, the submarine has been laying mines that can incapacitate the searching ship. As with each scenario, we defined a scenario-specific performance measure, in this case one whose value increases as a function of finding and destroying the submarine, as well as sweeping the mines. A non-GDA agent would ignore the mines because it would focus solely on its initial goal, whereas ARTUE would formulate a goal to sweep them. Table 2 displays our results for ARTUE and its ablations (i.e., which perform no GDA steps, only discrepancy detection, or only the first two steps,

TABLE 2 — Mean Performance Scores for the TAO Sandbox Scenarios

N = 25	Scouting	Iceberg	SubHunt
PLAN1	0.33	0.35	0.35
REPLAN	0.40	0.48	0.48
EXPLAIN	0.58	0.64	0.74
ARTUE	0.74	0.73	0.98

respectively). Analysis reveals significant performance differences between ARTUE and its ablations for all these scenarios.

Discussion: Our evaluations on the TAO Sandbox and other simulators involving multiple GDA agents have been encouraging.[2] However, many open research issues exist. For example, ARTUE requires a set of rules for triggering goal formulation during discrepancy resolution. We recently extended ARTUE to interactively acquire these rules and will soon study methods for automatically identifying events of interest to discrepancy detection. In an upcoming project, we will transition extensions of ARTUE for use in ICODES, a deployed system for ship cargo loading/unloading. Future plans also include examining its utility for controlling unmanned systems in complex maritime environments.

[Sponsored by NRL]

References

[1] M. Molineaux, M. Klenk, and D.W. Aha, "Goal-Driven Autonomy in a Navy Strategy Simulation," Proceedings of the Twenty-Fourth AAAI Conference on Artificial Intelligence, Atlanta, GA, July 11-15, 2010, pp. 1548–1554.

[2] H. Muñoz-Avila, U. Jaidee, D.W. Aha, and E. Carter, "Goal Driven Autonomy with Case-based Reasoning," Proceedings of the Eighteenth International Conference on Case-Based Reasoning, Alessandria, Italy, pp. 228–241 (Springer, Berlin, 2010).

Managing Multiple Radio Communications Channels

C. Wasylyshyn
Information Technology Division

Introduction: It is expected that future Naval forces will be defined by their agility and their capacity for coping with highly dynamic environments.[1] Decision-making in the Combat Information Center (CIC) of the future is exactly such an environment. The individual Naval watchstander might be responsible for the concurrent monitoring of numerous radio communications channels, along with actively monitoring and responding to events on multiple visual displays. Such attentionally demanding environments have motivated various human–computer interaction (HCI) solutions to help warfighters deal with the vast number of information sources needing to be monitored in order to perform their duties successfully.

Monitoring Multiple Communications Channels: Unlike reading, in which the information input rate can be controlled by one's eye movements, comprehension of speech is often dependent on a transient acoustic signal whose input rate is largely controlled by the speaker, not the listener. The information input rate, thus, is determined by the environment, and previous information is often not reviewable. In order to comprehend auditory information effectively, input must be analyzed, segmented, and processed for structure and meaning, all of which must occur even as new auditory information continues to arrive. When auditory input is rapid, listeners have even less time to carry out these integrative processes, and successful comprehension requires greater cognitive effort on the part of the watchstander.

This project addresses a critical consideration when designing HCI solutions in auditory display research: the limitations in watchstanders' abilities to attend to multiple, active communications channels. Instead of presenting messages that must be monitored in parallel, as is the current state of affairs in the CIC, listeners hear messages that are serialized and accelerated in order to facilitate better comprehension. In addition, this project explores the role of natural biases in human attention toward certain categories of information during the listening process. Building an effective system of synthetically accelerated voice communications requires the integration of insights from multiple disciplines including signal processing, cognitive psychology, and linguistics. Each of these disciplines has made and will continue to make contributions to the design and execution of our experiments.

Experimental Design: An auditory test bed was created with communications messages that were synthetically accelerated using a patented NRL speech-rate compression algorithm[2] known as pitch-synchronous segmentation (PSS). PSS retains the fundamental frequency of speech signals and preserves a high degree of intelligibility by representing speech as a combination of individual pitch waveforms that do not destructively interfere with one another. The PSS algorithm was used to construct synthetically accelerated communications messages for our experiments at rates ranging in 15% increments from 50% to 140% faster than normal.

The communications messages, themselves, were also structured to enhance comprehension. Based on theories of attention and memory,[3] the human attentional capacity is thought to be optimized for detecting relevant changes in the environment, or in this case, the communications message. These changes serve as natural cues to encode and later remember pertinent information. We, therefore, presented auditory information in a way that approximates how listeners more naturally perceive it, that is, by varying the number of natural cues contained in the message. It was expected that comprehension of messages that contained more of these natural cues would be better than comprehension of messages that contained fewer.

In order to assess the effectiveness of our design, we tested for training effects and practice effects when listening to accelerated speech, and examined whether the number of natural cues included in the messages would influence comprehension.

Results: Comprehension of auditory messages was compared at normal speed and at seven accelerated speech rates. Figure 4 shows data from one group assigned to a training condition compared to another group assigned to a condition where accelerated speech messages were presented in a random fashion. As can be seen in Fig. 4, overall comprehension for both groups declined as speech rate increased. Training was effective at slower accelerated speech rates (50% and 65% faster than normal). The optimum acceleration rate for comprehension, or the fastest rate at which speech can be presented so that performance does not

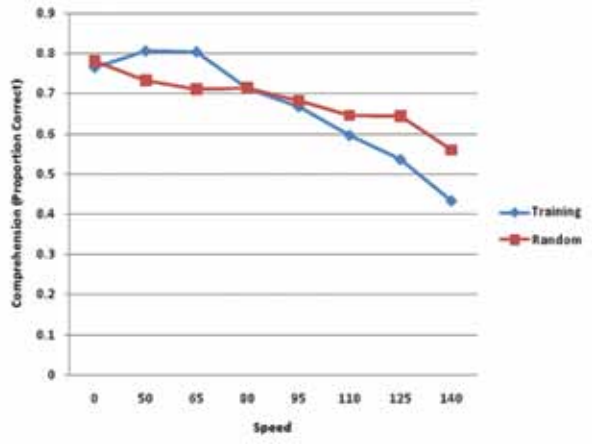

FIGURE 4
Comprehension (proportion correct) as a function of speed for the training and random presentation conditions. Note that 0 indicates normal speed speech; 50 to 140 denote % speed faster than normal.

differ from that at a normal rate, was 65% faster than normal. However, practice did not aid comprehension. That is, there was no systematic improvement shown after listening to multiple auditory messages presented at the same accelerated speech rate. Listeners simply adapted quickly when listening to accelerated speech. Structuring messages to contain more natural cues did enhance listeners' comprehension of information stated in the messages. This relationship is shown in Fig. 5.

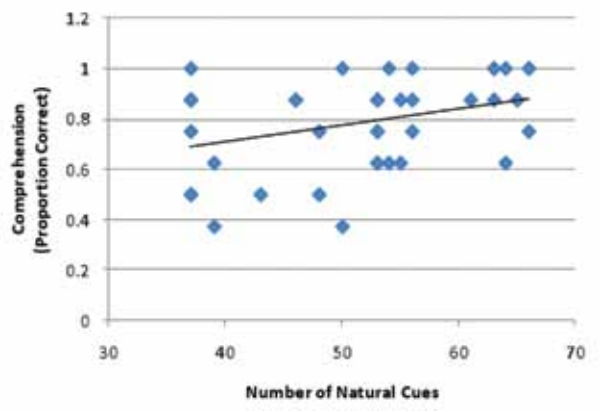

FIGURE 5
The relationship between comprehension (proportion correct) and the number of natural cues presented in the communications messages.

Summary: This research effort integrates several disciplines, including signal processing, cognitive psychology, and linguistics, in order to design a radio communications protocol that is minimally taxing to the watchstander and that will maximize the probability of message retention and understanding.

Acknowledgments: Many individuals have contributed to this effort. Particular thanks is due to Derek Brock, Wende Frost, LT Gregory Gibson, Brian McClimens, and Dennis Perzanowski (NRL). Thanks is also due to Paul Bello and Ray Perez (ONR).

[Sponsored by ONR]

References

[1] V. Clark, "Sea Power 21 Series - Part I: Projecting Decisive Joint Capabilities," *Naval Institute Proceedings Magazine* **128** (October 2002).

[2] G.S. Kang and L.J. Fransen, "Speech Analysis and Synthesis Based on Pitch-Synchronous Segmentation of the Speech Waveform," NRL/FR/5550--94-9743, Naval Research Laboratory, Washington, DC, 1994.

[3] J.M. Zacks and B. Tversky, "Event Structure in Perception and Conception," *Psychological Bulletin* **127**, 3–21 (2001).

Clutter Avoidance in Complex Geospatial Displays

M.C. Lohrenz[1] and M.R. Beck[2]
[1]*Marine Geosciences Division*
[2]*Louisiana State University*

Introduction: Clutter is a known problem in complex geospatial displays and can impact visual search and target detection performance. Set size (the number of distractors, i.e., features competing with the target for attention) and crowding (the amount of visual noise near the target) can predict search efficiency in displays with relatively simple features. However, set size and crowding can be difficult to measure in very complex displays.[1]

The authors recently introduced a measure of display clutter called the color-clustering clutter (C3) model, which correlates highly with subjective clutter ratings.[2] C3 measures clutter as a function of color density and saliency. Color density is determined by clustering all pixels in an image by location and color and calculating, for each cluster, the number of clustered pixels divided by the cluster area. Higher density implies lower clutter, because similarly colored pixels are packed more closely together, giving an impression of less complexity. Saliency is calculated as the difference in color between each cluster and all adjacent clusters. High saliency in a region with low density predicts the greatest clutter (see Ref. 2 for more details about C3).

Beck et al.[1] demonstrated that at least two interacting measures of clutter (using C3) are needed to (1) predict target detection performance (measured as response time) and (2) model limitations on attention during visual search of complex displays. These two measures are global clutter (the average clutter of the entire display) and local clutter (the clutter immediately surrounding the target). The authors found that, in

complex geospatial displays, global clutter can represent set size, and local clutter can represent crowding, both of which impact the limits on attention during visual search.

In an effort to better understand the effects of clutter on visual search and target detection performance, the authors examined search strategies by tracking the pattern of eye movements. They found that people tend to start searching in less cluttered areas and progress to more cluttered areas as needed to find a target.[3] The authors designed a follow-on experiment to test and validate that claim, the results of which are published here.

Method: Forty-two undergraduates from the Louisiana State University (LSU) participated for course credit. Stimuli were cropped sections (740 × 580 pixels) of digital aeronautical charts. Thirty-six charts were selected such that their global C3 values were equally spaced from the least-cluttered chart (#1, C3 = 0.95) to the most-cluttered chart (#36, C3 = 9.29). Two versions of each chart were created: one with a target in a relatively low local-clutter area of the chart, and the other with a target in a relatively high local-clutter area. In each case, the target was a single-bump obstacle symbol (17 × 16 pixels) randomly overlaid on the charts.

Charts were presented on a 19-in. CRT monitor. Subjects rested their heads in a chin rest 40 cm from the screen. An EyeLink II (SR Research Ltd.) eye tracker presented the stimuli in random order and recorded key presses and eye movement data, including saccades and fixations. A saccade is detected when eye movement velocity is more than 30 degrees per second, and a fixation is detected when eye movement velocity is below this threshold. Subjects fixated on a dot in the center of the screen and pressed a key to begin. For each trial, a chart was presented, and subjects found the target as quickly as possible, pressing a button to indicate they had found it.

A fixation was considered to be on the target if it was within 36 pixels (2° visual angle) of the target. Otherwise, the fixation was said to be on some other, non-target feature. Local C3 values were calculated for 60 × 60 pixel sections of the charts centered on each non-target fixation, excluding the initial center-point fixation for each trial and all fixations after the subject found the target.

Results: Figure 6 (top) presents normalized C3 clutter (relative to global clutter) for non-target fixations, averaged by fixation index (where #1 is the first fixation in a given trial) across all subjects and all charts. The average number of fixations per trial was 50.2, and the median was 19.5, ranging from 1 to 403. Fixation #1 is excluded, since it was constrained to be at the center of the display. The average local clutter of fixated regions first drops sharply ($R = -0.97$; $R^2 = 0.94$) from fixations #2 through #4, as subjects direct their attention away from the center point. Figure 6 (bottom) shows that the locations of these first few fixations are strongly influenced by the central starting point.

After fixation #4, however, the average clutter of fixated regions steadily increases, suggesting subjects tend to move from less cluttered regions of the display to progressively more cluttered regions until finding the target (Fig. 6, top). The last fixation index included in the analysis is fixation #24 because there were fewer than 50% of participants with fixation indexes higher than 24. The correlation between average fixation clutter and fixation index for fixations #4 through #24 is 0.93 ($R^2 = 0.87$). These findings are consistent with (and stronger than) those from Lohrenz and Beck.[3]

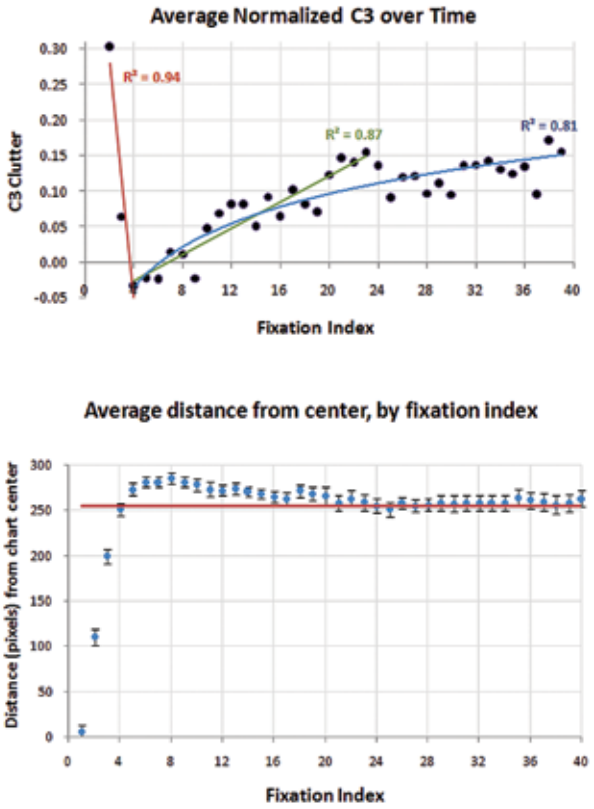

FIGURE 6
Top: The local clutter value for fixated regions of the chart (averaged by fixation index) drops sharply at the beginning of trials (fixations #2 through #4), then gradually increases as the search proceeds.The effect tapers off as fewer participants are left in a trial. Fixation #24 is the last fixation index for which at least 50% of participants fixated, on average. Bottom: The distance of fixations from the center of the chart (averaged by fixation index, across all subjects and charts) shows that the locations of the first four fixations of each trial are strongly influenced by the central starting point. The maximum possible distance from the center of the chart to a fixation (i.e., in a chart corner) is 470 pixels. Error bars represent 2 standard errors of the mean.

Examination of eye movements during this search task also reveals that participants were using a "coarse-to-fine" search strategy in charts of all levels of clutter; as search progresses, the duration of fixations increases, while saccade distance (between adjacent fixations) decreases (Fig. 7). This "coarse-to-fine" search strategy is not necessarily the most efficient. The authors found that participants using a global attention strategy (fewer and longer fixations) from the start of a trial found the target faster, especially in the high local-clutter condition (Fig. 8). However, this strategy was not typically seen until later in a trial (Fig. 7).

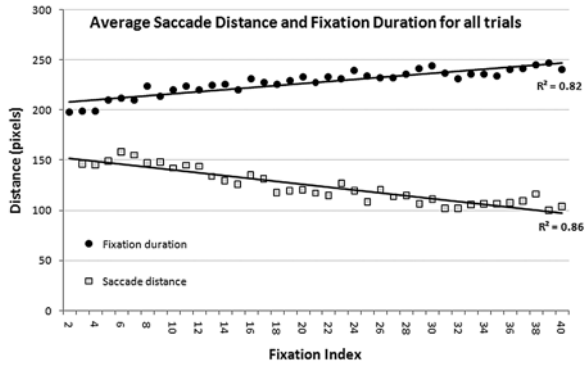

FIGURE 7
Participants used a "coarse-to-fine" search strategy in charts of all levels of clutter; as search progressed, the duration of each fixation increased and the distance between fixations decreased.

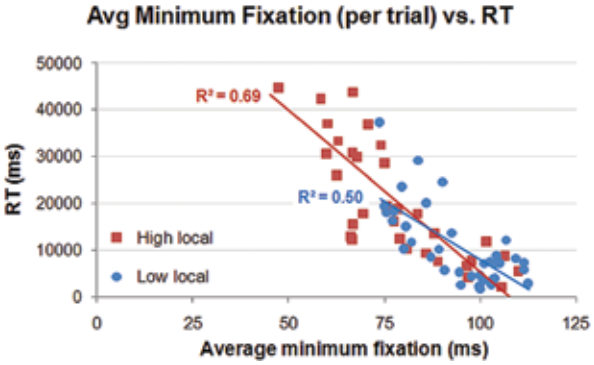

FIGURE 8
Participants with longer minimum fixations found the target faster, suggesting that a global attention strategy (longer and fewer fixations) was more efficient, especially in the more difficult high local-clutter condition.

Conclusions: This report describes several visual search strategies observed in participants during a target detection task with complex aeronautical charts. Participants tended to initially seek out less cluttered regions of the chart to begin their search, only searching in more cluttered regions if needed to find the target. These results validate earlier experiments.[3]

Likewise, at the start of trials, participants tended to use shorter fixations and longer saccades (i.e., quickly refocusing attention to different parts of the chart), and gradually transitioned to longer fixations with shorter saccades as the trial progressed. This is not the most efficient search strategy, however, since participants who tended to use fewer and longer fixations throughout a trial found the target faster. This suggests that it might be possible to train people to be more efficient searchers by training their patterns of eye movements.

Acknowledgments: We thank the LSU Psychology Department for computer resources and students to participate in the clutter experiments, and Amanda van Lamsweerde at LSU for administering the trials. We also thank Stephanie Myrick at NRL for her assistance in collecting the digital aeronautical charts for this study.

This article is dedicated to the memory of our friend and colleague, Dr. Marlin L. Gendron. Marlin contributed his priceless insights and creative energy to this and countless other research projects during his 15 years with NRL.

[Sponsored by NRL]

References

[1] M.R. Beck, M.C. Lohrenz, and J.G. Trafton, "Measuring Search Efficiency in Complex Visual Search Tasks: Global and Local Clutter," *Journal of Experimental Psychology: Applied* **16**(3), 238–250 (2010).

[2] M.C. Lohrenz, J.G. Trafton, M.R. Beck, and M.L. Gendron, "A Model of Clutter for Complex, Multivariate, Geospatial Displays," *Human Factors* **51**(1), 90–101 (2009).

[3] M.C. Lohrenz and M.R. Beck, "Evidence of Clutter Avoidance in Complex Scenes," Proceedings of the Human Factors and Ergonomics Society 54th Annual Meeting, San Francisco, CA, September 2010, pp. 1355–1359.